

We are IntechOpen, the world's leading publisher of Open Access books Built by scientists, for scientists

6,900

Open access books available

186,000

International authors and editors

200M

Downloads

Our authors are among the

154

Countries delivered to

TOP 1%

most cited scientists

12.2%

Contributors from top 500 universities



WEB OF SCIENCE™

Selection of our books indexed in the Book Citation Index
in Web of Science™ Core Collection (BKCI)

Interested in publishing with us?
Contact book.department@intechopen.com

Numbers displayed above are based on latest data collected.
For more information visit www.intechopen.com



Growth of Organic Nonlinear Optical Crystals from Solution

A. Antony Joseph and C. Ramachandra Raja
*Department of Physics, Government Arts College (Autonomous),
Kumbakonam, Tamil Nadu,
India*

1. Introduction

Investigations on the growth of good quality single crystals play an important role in the development of modern scientific world with advanced technology. Behind the development in every new solid state device and the explosion in solid state device, there stands a single crystal. Crystal growth is an important field of materials science, which involves controlled phase transformation. In the past few decades, there has been a growing interest in crystal growth process, particularly in view of the increasing demand for materials for technological applications (Brice, 1986). Researchers worldwide have always been in the search of new materials and their single crystal growth.

Solids exist in two forms namely single crystals, polycrystalline and amorphous materials depending upon the arrangement of constituent molecules, atoms or ions. An ideal crystal is one, in which the surroundings of any atom would be exactly the same as the surroundings of every similar atom. Real crystals are finite and contain defects. However, single crystals are solids in the most uniform condition that can be attained and this is the basis for most of the uses of these crystals. The uniformity of single crystals can allow the transmission without the scattering of electro magnetic waves. The methods of growing crystals are very wide and mainly dictated by the characteristics of the material and its size (Buckley, 1951).

2. Nucleation

Comprehensive study on the growth of crystals should start from an understanding of nucleation process. Nucleation is the process of generating within a metastable phase, initial fragments of a new and more stable phase. In a supersaturated or super-cooled system when a few atoms or molecules join together, a change in energy takes place in the process of formation of the cluster. The cluster of such atoms or molecules is termed as "embryo". An embryo may grow or disintegrate and disappear completely. If the embryo grows to a particular size, critical size known as 'critical-nucleus' then greater is the possibility for the nucleus to grow into a crystal. Thus nucleation is an important event in crystal growth.

2.1 Kinds of nucleation

Nucleation is broadly classified into two types. These two types are frequently reserved to as primary and secondary nucleation. The former occurs either spontaneously or induced

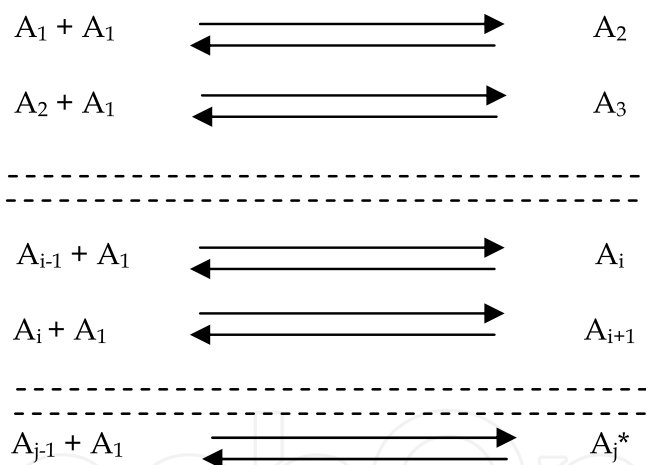
artificially. The spontaneous formation of crystalline nuclei within the interior of parent phase is called homogeneous nucleation. On the other hand if the nuclei form heterogeneously around ions, impurity molecules or on dust particles or on surface of the container or at structural singularities such as dislocation or imperfection, it is called heterogeneous nucleation. If the nuclei are generated in the vicinity of crystals present in supersaturated system then this phenomenon is often referred to as "secondary" nucleation. Nucleation can often be induced by external influence like agitation, mechanical shock, friction, spark, extreme pressure, electric and magnetic fields, UV -rays, X-rays, gamma rays and so on.

2.2 Classical theory of nucleation

The formation of the crystal nuclei is a difficult and a complex process, because the constituent atoms or molecules have to be oriented into a fixed lattice. In practice, a number of atoms or molecules may come together as a result of statistical incidence to form an ordinary cluster of molecules known as embryo.

2.3 Kinetic theory of nucleation

The main aim of the nucleation theory is to calculate the rate of nucleation. Rate of nucleation is nothing but the number of critical nuclei formed per unit time per unit volume. In kinetic theory, nucleation is treated as the chain reaction of monomolecular addition to the cluster and ultimately reaching macroscopic dimensions is represented as follows:



Two monomers collide with one another to form a dimer. A monomer joins with a dimer to form a trimer. This reaction builds a cluster having i -molecules known as i -mer. As the time increases the size distribution in the embryos changes and larger ones have increase in size. As the size attains a critical size A_j^* , the further growth into macroscopic size is guaranteed, as there is a possibility for the reverse reaction i.e., the decay of a cluster into monomers.

3. Stability of nucleus

An isolated droplet of a fluid is most stable when its surface free energy and therefore its area is a minimum. According to Gibbs (Gibbs & Longmans, 1982), the total free energy of a crystal in equilibrium would be minimum for a given volume if its surrounding is at constant temperature and pressure.

If the volume free energy per unit volume is considered to be constant then,

$$\sum a_i \sigma_i = \text{minimum} \quad (1)$$

Where, a_i is the area of i^{th} face and σ_i is the corresponding surface energy per unit area.

4. Energy formation of spherical nucleus

The total free energy change associated with the process of homogenous nucleation shall be considered as follows. Let ΔG be the overall excess free energy of an embryo between the two phases mentioned above. ΔG can be represented as a combination of volume and surface energies since an embryo possesses both these energies.

$$\Delta G = \Delta G_s + \Delta G_v \quad (2)$$

Where, ΔG_s is the surface excess free energy and ΔG_v is the volume excess free energy. Assuming the second phase to be spherical.

$$\Delta G = 4 \pi r^2 \sigma + 4/3 \pi r^3 \Delta G_v \quad (3)$$

Where ΔG_v is the free energy change per unit volume is a negative quantity and ' σ ' is the free energy change per unit area. The quantities ΔG , ΔG_s and ΔG_v are represented in Fig 1. The surface excess free energy increases with r^2 and the volume excess free energy decreases with r^3 so the total free energy change increases with increase in size of the nucleus and attains a maximum and then decreases for further increase in the size of nucleus. The size corresponding to the nucleus in which the free energy change is maximum is known as the critical size and can be obtained mathematically by maximizing the equation (3).

$$\text{i.e.,} \quad \frac{d\Delta G}{dr} = 0$$

Or

$$\frac{d\Delta G}{dr} = 8\pi r\sigma + 4\pi r^2 \Delta G_v = 0$$

When $r = r^*$ (radius of critical nucleus), simplifying we have

$$r^* = -2\sigma / \Delta G_v \quad (4)$$

The free energy change associated with the formation of critical nucleus can be estimated by substituting equation (4) in equation (3)

$$\Delta G^* = 16 \pi \sigma^3 / 3 \Delta G_v^2 \quad (5)$$

$$G^* = 4/3 \pi r^{*2} \sigma$$

$$\Delta G^* = 1/3 S.\sigma \quad (6)$$

Where ' S ' is the surface area of the critical nucleus. Though the present phase is at constant temperature and pressure, there will be variation in the energies of the molecules. The molecules having higher energies temporarily favour the formation of the nucleus. The rate of nucleation can be given by Arrhenius reaction which is a velocity equation since the nucleation process is basically a thermally activated process. The nucleation rate J is given by

$$J = A \exp \left\{ \frac{-\Delta G^*}{KT} \right\} \quad (7)$$

Where, 'A' is the pre-exponential constant, 'K' is the Boltzman constant and 'T' is the absolute temperature.

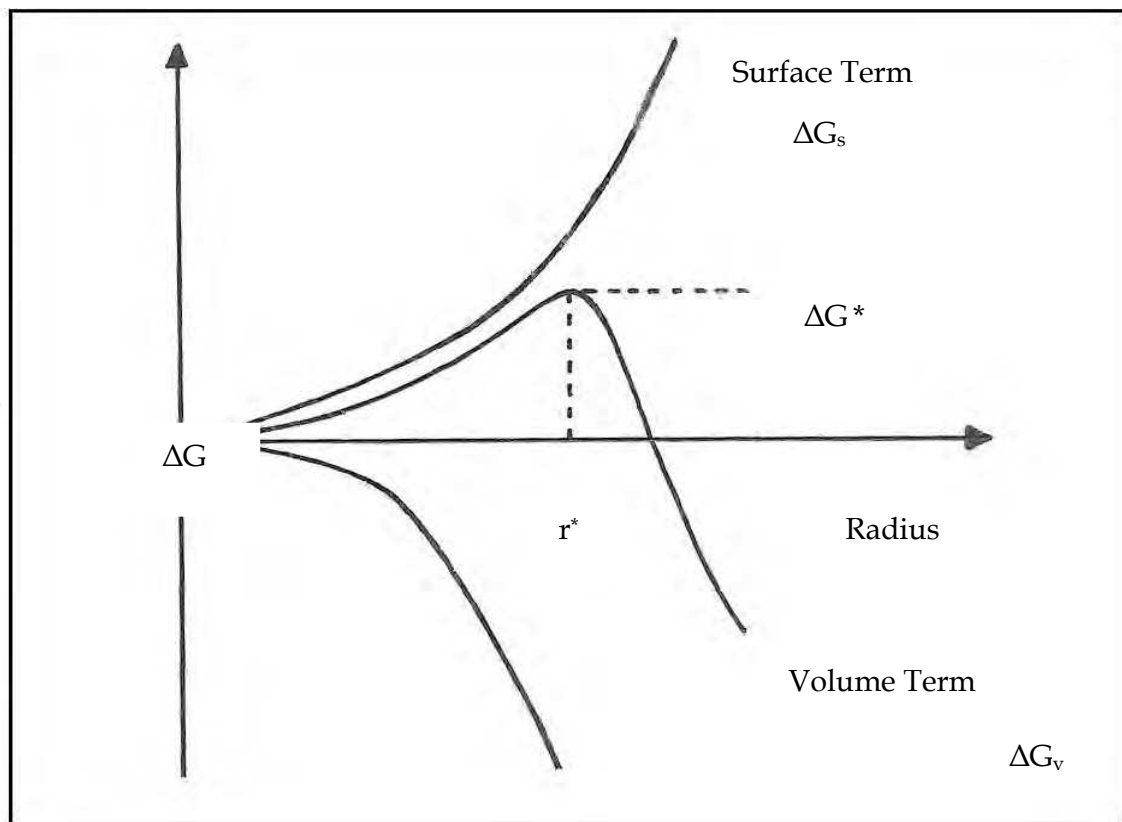


Fig. 1. Free energy diagram.

5. Classification of crystal growth

The growth of the single crystal developed over the years to satisfy the needs of modern technology. The free energy of the growing crystal must be lower than initial stage of the system. It is the common condition for all crystal growth process. The crystal growth method is classified into three types namely growth from melt, from vapour, from the solution. The selection method of crystal growth depending upon the physical properties of material

- Growth from solid -----> solid-solid phase transformation
- Growth from liquid -----> liquid-solid phase transformation
- Growth from vapour -----> vapour-solid phase transformation

We can consider the conversion of the polycrystalline piece of a material into a single crystal by causing the grain boundaries to sweep through and pushed out of the crystal in the solid-solid growth of crystals. The crystal growth from liquid falls into four categories namely,

- i. Gel growth,
- ii. Flux growth,
- iii. Hydrothermal growth and
- iv. Low temperature solution growth.

Low temperature solution growth is the most widely practiced next to growth from melt. Crystal growth from solution always occurs under condition in which the solvent and crystallizing substance interact. The expression "solution" is most commonly used to describe the liquid which is the result of dissolving a quantity of given substance in a pure liquid known as solvent. Usually water is used as the solvent rarely other liquid is also used as solvent.

6. Solvent selection

The solution is a homogeneous mixture of a solute in a solvent. Solute is the component present in a smaller quantity. For a given solute, there may be different solvents. Apart from high purity starting materials, solution growth requires a good solvent. The solvent must be chosen taking into account the following factors:

1. A good solubility for the given solution.
2. A positive temperature co-efficient of solubility.
3. A small vapour pressure.
4. Non-corrosiveness.
5. Non-flammability.
6. Less viscosity.
7. Low price in the pure state.

7. Solution preparation and crystal growth

After selecting the desirable solvent with high purity solute to be crystallized, the next important part is preparation of the saturated solution. To prepare a saturated solution, it is necessary to have an accurate solubility-temperature data of the material. The saturated solution at a given temperature is placed in the constant temperature bath. Whatman filter papers are used for solution filtration. The filtered solution is taken in a growth vessel and the vessel is sealed by polythene paper in which 10-15 holes were made for slow evaporation. This solution was transferred to crystal growth vessels and crystallization is allowed to take place by slow evaporation at room temperature or at a higher temperature in a constant temperature bath. As a result of slow evaporation of solvent, the excess of solute which got deposited in the crystal growth vessel results in the formation of seed crystals.

8. Low temperature solution growth methods

Solution growth is the most widely used method for the growth of crystals, when the starting materials are unstable at high temperatures. In general, this method involves seeded growth from a saturated solution. The driving force i.e., the supersaturation is achieved either by temperature lowering or by solvent evaporation. This method is widely used to grow bulk crystals, which have high solubility and have variation in solubility with temperature (James & Kell, 1975).

Low temperature solution growth (LTSG) can be subdivided into the following categories:

- i. Slow cooling method
- ii. Slow evaporation method
- iii. Temperature gradient method

8.1 Slow cooling method

In this process, supersaturated solution is prepared by keeping quantity of the solution same as that of the initial stage and temperature of the solution is reduced in small step. By doing so, solution which is just saturated at initial temperature will become supersaturated solution. Once supersaturation is achieved, growth of single crystal is possible. The main disadvantage of slow cooling method is the need to use a range of temperature. Wide range of temperature may not be desirable because the properties of the grown crystal may vary with temperature. Even though this method has technical difficulty of requiring a programmable temperature control, it is widely used with great success.

8.2 Slow evaporation method

In this process the temperature of the solution is not changed, but the solution is allowed to evaporate slowly. Since the solvent evaporates, concentration of solute increased and therefore supersaturation is achieved. For example 40 g of solute in 100 ml solvent is considered as saturated solution at 50°C. Now the solution is allowed to evaporate at the same temperature. The 100 ml of the solution is reduced to some lower level say 70 ml. Then 40 g in 70 ml at 50°C is supersaturated solution. The evaporation technique has an advantage that the crystals grow at a fixed temperature. But inadequacies of the temperature control system still have a major effect on the growth rate. This method can effectively be used for materials having very low temperature coefficient of solubility.

8.3 Temperature gradient method

This method involves the transport of the materials from hot region containing the source materials to be grown to a cooler region, where the solution is supersaturated and the crystal grows. The advantages of this method are that [a] the crystal is grown at fixed temperature, [b] this method is insensitive to changes in temperature provided both the source and the growing crystal under go the same change. [c] economy of the solvent. On the other hand, small changes in temperature difference between the source and the crystal zones have a large effect on the growth rate.

In general, crystal growth from solution is mainly influenced by super saturation. Super saturation may be achieved by any methods (described above) which are based on the principle that solution which is saturated at a particular temperature will behave as unsaturated at high temperature. The disadvantages are the slow growth rate and in many cases inclusion of the solvent in to the growing crystal. Materials having moderate to high solubility in temperature range, ambient to 100°C at atmospheric pressure can be grown by LTSG method. This method is well suitable for those materials which suffer from decomposition in the melt and which undergo structural transformation while cooling from the melting point. The other advantages of LTSG method are the low working temperature, easy operation and feasible growth condition.

9. Nonlinear optical crystals

Non Linear optics deals with the interaction of intense electromagnetic fields in suitable medium producing magnified fields different from the input field in frequency, phase or amplitude Nonlinear optics is now established as an alternative field to electronics for the future photonic technologies. The fast-growing development in optical fiber communication

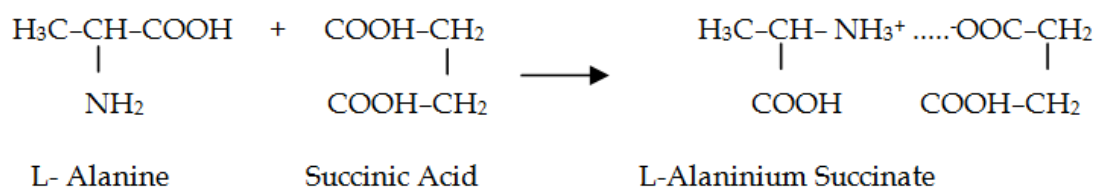
systems has stimulated the search for new highly nonlinear materials capable of fast and efficient processing of optical signals. Organic nonlinear optical (NLO) materials have been intensely investigated due to their potentially high nonlinearities and rapid response in electro-optic effect compared to inorganic NLO materials. In recent years, there has been considerable interest in the study of organic NLO crystals with good nonlinear properties because of their wide applications in the area of laser technology, optical communication, optical information processing and optical data storage technology (Chenthamarai et al., 2000). Among the organic crystals for NLO applications, amino acids display specific features of interest such as (i) molecular chirality, which secures acentric crystallographic structures, (ii) absence of strongly conjugated bonds, leading to wide transparency ranges in the visible and UV spectral regions, (iii) Zwitterionic nature of the molecule, which favours crystal hardness. Further they can be used as a basis for synthesizing organic compounds and derivatives (Eimerl et al., 1990). In our laboratory, we have grown NLO crystals such as L-Alaninium Succinate (LAS), L-Valinium Succinate (LVS), L-Alaninium Fumarate (LAF), L-Valinium Fumarate (LVF) and reported in the journal of repute (Ramachandra Raja, 2009a, 2009b, 2009c, 2010).

In this chapter, we have discussed the growth of organic nonlinear optical crystal. L-Alaninium Succinate (LAS) and L-Valinium Succinate (LVS) which have been grown by slow evaporation solution growth technique in detail. The characteristic studies such as single crystal and powder X-ray Diffraction (XRD) analysis, UV-Vis-NIR spectrum, FT-IR, nuclear magnetic resonance studies, TGA/DTA studies and SHG are also discussed.

10. Growth and characterization of L- Alaninium Succinate (LAS)

10.1 Crystal growth

LAS have been grown from aqueous solution by slow evaporation. The starting material was synthesized from commercially available L-Alanine (AR grade) and Succinic acid (AR grade), taken in the equimolar ratio 1:1. In deionized water, L-Alanine and Succinic acids were allowed to react by the following reaction to produce LAS.



Calculated amount of the reactants were thoroughly dissolved in deionized water and stirred well for about 3 hours using a magnetic stirrer to obtain a homogenous mixture. Then the solution was allowed to evaporate slowly until the solvent was completely dried. The purity of the synthesized salt was further increased by successive recrystallization process. The synthesized powder of LAS was dissolved thoroughly in double distilled water to form a saturated solution. The solution was then filtered twice to remove any insoluble impurities. Growth was carried out by low-temperature solution growth technique by slow evaporation in a constant temperature bath controlled to an accuracy of $\pm 0.01^\circ\text{C}$. Crystals begin to grow inside the solution and were removed from the solution after 3 weeks, washed and dried in air.

10.2 Characterization studies

10.2.1 Single crystal XRD analysis

In order to estimate the crystal data, the single crystal XRD analysis of grown LAS crystal have been carried out using ENRAF NONIUS CAD-4 X-ray diffractometer equipped with MoK α ($\lambda = 0.71069 \text{ \AA}$) radiation. The X-ray diffraction study on grown crystal reveals that the grown crystal belongs to orthorhombic system with the following unit cell parameters: $a = 5.77 \text{ \AA}$, $b = 6.02 \text{ \AA}$, $c = 12.32 \text{ \AA}$ and $\alpha = \beta = \gamma = 90^\circ$, the cell volume = 428 \AA^3 . These lattice parameters are tabulated in the Table 1.

10.2.2 Powder XRD analysis

The structural property of the single crystals of LAS has been studied by X-ray powder diffraction technique. Powder X-ray diffraction studies of LAS crystal is carried out, using Rich Seifert diffractometer with CuK α ($\lambda = 1.54060 \text{ \AA}$) radiation. The sample is scanned for 2θ values from 10° to 90° at a rate of $2^\circ/\text{min}$. Figure 2 shows the Powder XRD pattern of the pure LAS crystal. The diffraction pattern of LAS crystal has been indexed by Reitveld index software package. The lattice parameter values of LAS crystal has been calculated by Reitveld unit cell software package and are matched with single crystal XRD data. The comparison of lattice parameters between single crystal and powder XRD is shown in Table 1.

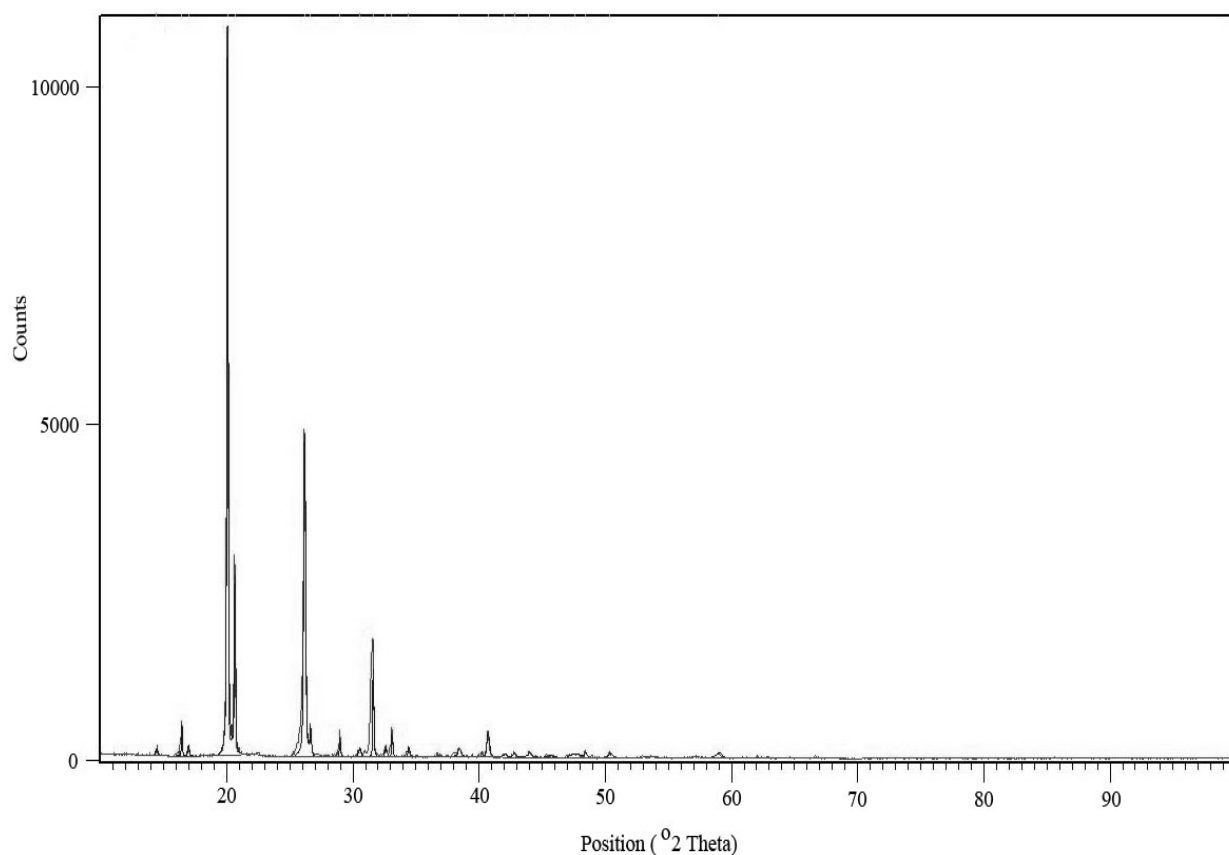


Fig. 2. Powder XRD pattern of LAS crystal.

XRD	a Å	b Å	c Å	α deg	β deg	γ deg	Volume Å ³
Single crystal	5.77	6.02	12.32	90	90	90	428
Powder	5.74	5.98	12.53	90	90	90	430

Table 1. The cell parameters of LAS crystal.

Position 2θ	d- spacing Å	(h k l)
14.4335	6.13689	(0 0 2)
16.4368	5.39317	(0 1 1)
16.9673	5.22574	(1 0 1)
20.0604	4.42642	(0 1 2)
20.6379	4.30384	(1 0 2)
26.1583	3.40675	(0 1 3)
26.6351	3.34684	(1 0 3)
28.9666	3.08254	(0 0 4)
30.5183	2.92926	(1 1 3)
31.5955	2.83181	(2 0 1)
32.5805	2.74841	(0 1 4)
33.0863	2.70753	(0 2 2)
34.4077	2.60652	(2 1 0)
38.4281	2.34257	(2 0 3)
40.6932	2.21726	(1 2 3)
42.0137	2.15057	(0 2 4)
42.789	2.11339	(2 0 4)
43.9448	2.06045	(2 2 1)
45.5981	1.98951	(2 1 4)
47.5815	1.91111	(0 3 2)
48.4142	1.88017	(2 0 5)
50.3422	1.81259	(1 2 5)
58.9467	1.56559	(3 2 2)

Table 2. Powder XRD data of LAS crystal.

It is observed that LAS belongs to orthorhombic system and cell parameters values are in good agreement with the single crystal XRD data. The h, k, l values, d-spacing and 2θ values are tabulated in Table 2.

10.2.3 UV-Vis-NIR analysis

The UV-Vis-NIR transmittance spectrum of grown LAS crystal has been recorded with a Lambda 35 double-beam spectrophotometer in the range 190–1100 nm to find the suitability of LAS crystal for optical applications. The recorded spectrum is shown in Fig. 3. The crystal shows a good transmittance in the visible region which enables it to be a good material for optoelectronic applications. As observed in the spectrum, there is no significant absorption in the entire range tested. A good optical transmittance from ultraviolet to infrared region is very useful for nonlinear optical applications. Most of the nonlinear optical effects are studied using Nd:YAG laser operating at a fundamental wavelength of 1064 nm. Absorption, if any, near the fundamental or the second harmonic at 532 nm, will lead to a loss of conversion efficiency of second harmonic generation (SHG). From the UV-Vis-NIR spectrum, it is clear that the transparency of the grown crystals extends up to UV region.

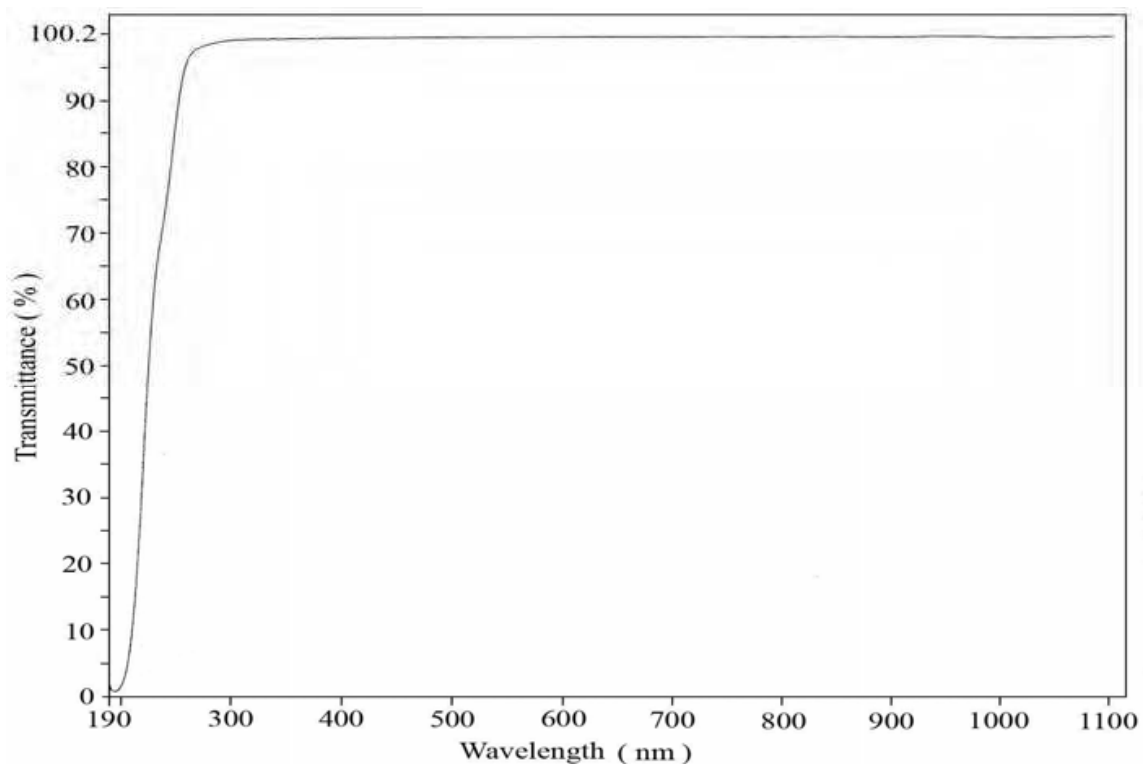


Fig. 3. Transmission spectrum of LAS crystal.

The lower cut-off wavelength is as low as 190 nm. The wide range of transparency suggests that the crystal is a good candidate for nonlinear optical applications (Aravindan et al., 2007). This transmittance window (190–1100 nm) is sufficient for the generation of second harmonic light ($\lambda = 532$ nm) from the Nd:YAG laser ($\lambda = 1064$ nm) (Natarajan et al., 2008). The lower cut-off near 190 nm combined with the very good transparency, makes the usefulness of this material for optoelectronic and nonlinear optical applications.

10.2.4 FT-IR analysis

The infrared spectrum of LAS has been carried out to analyse the chemical bonding and molecular structure of the compound. The FT-IR spectrum of the crystal has recorded in the

frequency region from 400 cm^{-1} to 4000 cm^{-1} with Perkin-Elmer FT-IR spectrometer model SPECTRUMRX1 using KBr pellets containing LAS powder obtained from the grown single crystals. The observed FT-IR spectrum of LAS is as shown in Fig. 4.

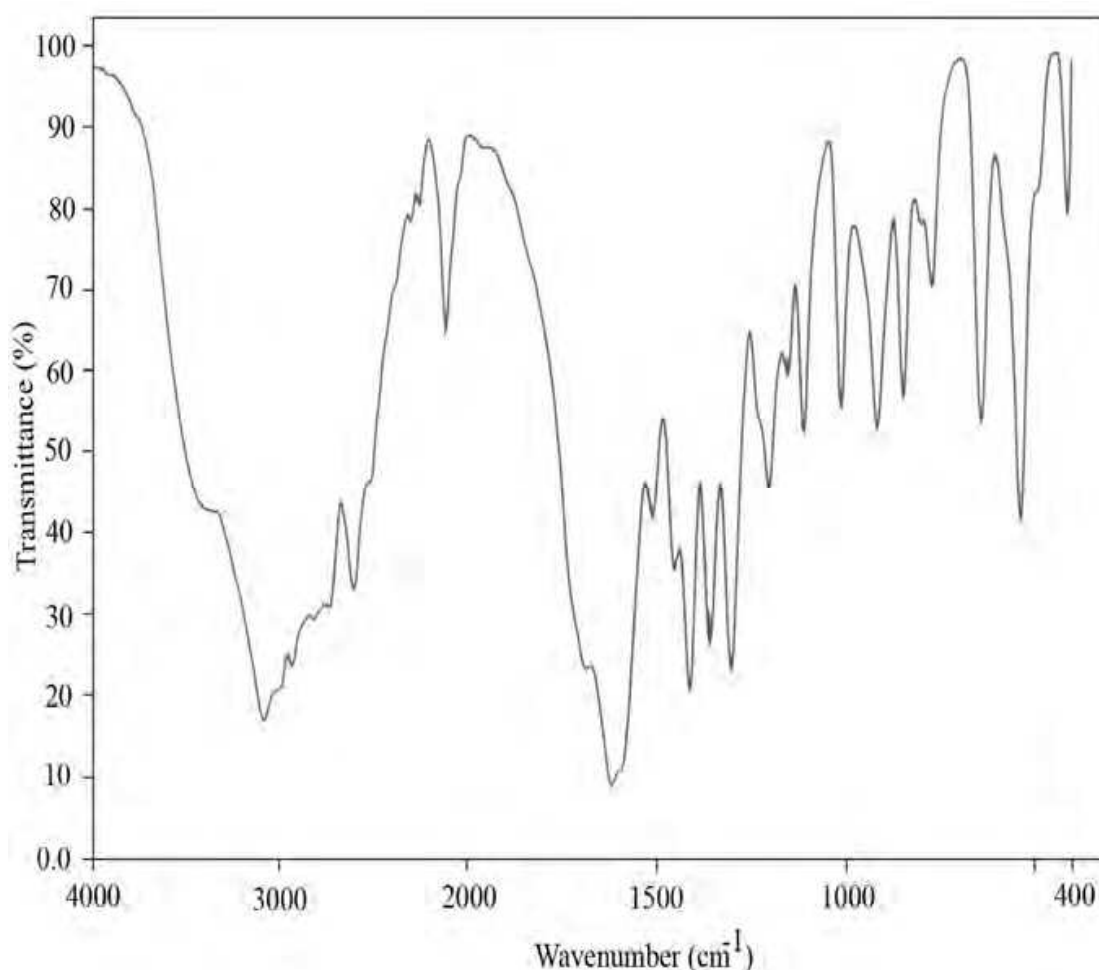


Fig. 4. FT-IR spectrum of LAS crystal.

The characteristics vibration of LAS has been compared with L-alaninium alanine nitrate (Aravindan et al., 2007) and L-alanine cadmium chloride (Dhanuskodi et al., 2007) as shown in Table 3. The asymmetric stretching vibration of NH_3^+ is observed at 3086 cm^{-1} of LAS is confirming the presence of NH_3^+ in compound. The NH_3^+ absorption range of amino acids ($3130\text{--}3100\text{ cm}^{-1}$) is shifted to lower wave number, due to formation of amino salts, and in LAS, it is observed at 3086 cm^{-1} .

Amino group absorption bands are noted at 2604 cm^{-1} (symmetric stretching), 1620 cm^{-1} (bending), and 1111 cm^{-1} (rocking). These bands are due to NH_3^+ ions. During the formation of amino salts, the NH_2 group in amino acids is converted in to NH_3^+ ion. The strong absorption at 1413 cm^{-1} indicates the symmetric stretching vibration frequency of carbonyl group. The bending and rocking vibrations of COO^- are observed at 772 cm^{-1} and 539 cm^{-1} , respectively. CH_2 wagging (1304 cm^{-1}) and CH_3 stretching (1204 cm^{-1}) vibrations are also observed (Ramachandran & Natarajan, 2007).

Wavenumber (cm^{-1})	Assignment
3086	NH_3^+ asymmetric stretching
2604	NH_3^+ symmetric stretching
1620	NH_3^+ bending
1453	CH_3 bending
1413	COO^- symmetric stretching
1360	CH_3 symmetric bending
1304	CH_2 wagging
1204	CH_3 symmetric stretching
1111	NH_3^+ rocking
1012	CH_3 rocking
917	CCN symmetric stretching
848	C-CH_3 bending
772	COO^- bending
539	COO^- rocking
412	COO^- rocking

Table 3. Assignments of FT-IR bands observed for LAS crystal.

10.2.5 NMR studies

The ^1H - and ^{13}C -NMR spectra of LAS have been recorded using D_2O as solvent on a Bruker 300MHz (Ultrashield) TM instrument at 23°C (300 MHz for ^1H -NMR and 75 MHz for ^{13}C -NMR) to confirm the molecular structure. The spectra are shown in Figures 5 and 6 respectively and the chemical shifts are tabulated with the assignments in Table 4.

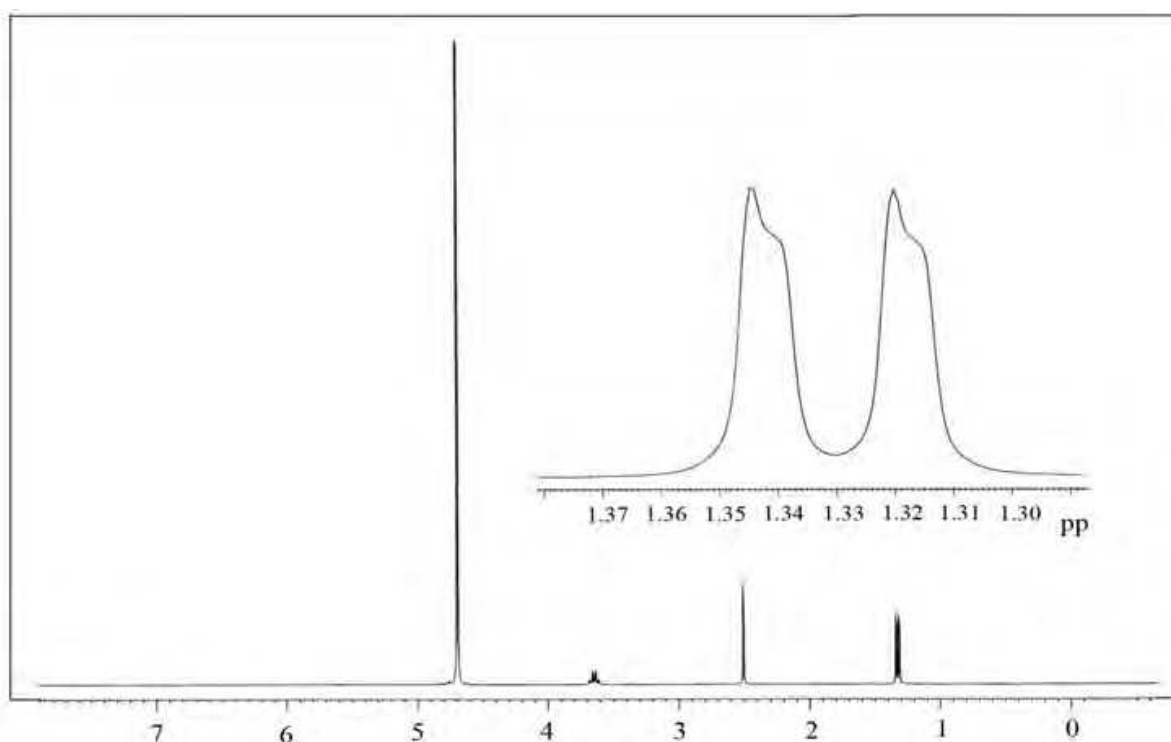


Fig. 5. ^1H -NMR spectrum of LAS crystal.

The resonance peaks at $\delta = 1.33$ ppm of $^1\text{H-NMR}$ spectrum is due to the CH_3 group and peaks observed at $\delta = 3.65$ ppm is due to the CH group of L-Alanine. The methyl proton signal at $\delta = 1.33$ ppm is split into a proton doublet due to the coupling of the neighboring proton (CH) and the signal at $\delta = 3.65$ ppm is split into a proton quartet due to the coupling of three neighboring protons (CH_3). The resonance peak observed as a singlet at $\delta = 2.57$ ppm exhibits the presence of methylene (CH_2) proton of succinic acid.

The signal at $\delta = 4.69$ ppm is due to the solvent (D_2O). The signals due to NH and COOH do not show up because of fast deuterium exchange reactions takes place in these two groups, with D_2O being used as solvent (Bruice, 2002). Because of the presence of the methylene (CH_2) groups of LAS, electron contributions towards the rest of the compound get enhanced, so that the protons are more protected in LAS. Such property is not noticed in L-alaninium oxalate (LAO), due to the absence of methylene groups so that the proton groups in LAS absorbs signals at the values lesser than the value of LAO (Dhanuskodi & Vasantha, 2004). The ^{13}C NMR spectrum of LAS contains five signals. The resonance peaks observed at $\delta = 16.00$ ppm and at $\delta = 50.33$ ppm are due to the carbon environments of CH_3 and CH groups of L-alanine respectively. The signal at $\delta = 29.06$ ppm is due to the presence of two methylene (CH_2) groups of succinic acid. The resonance signal observed at $\delta = 175.52$ ppm is due to the free carboxylic acid from L -alanine. In solution, the two carboxyl groups of succinic acid are equivalent due to the fast exchange of H^+ between them and give rise to a single signal at $\delta = 177.41$ ppm.

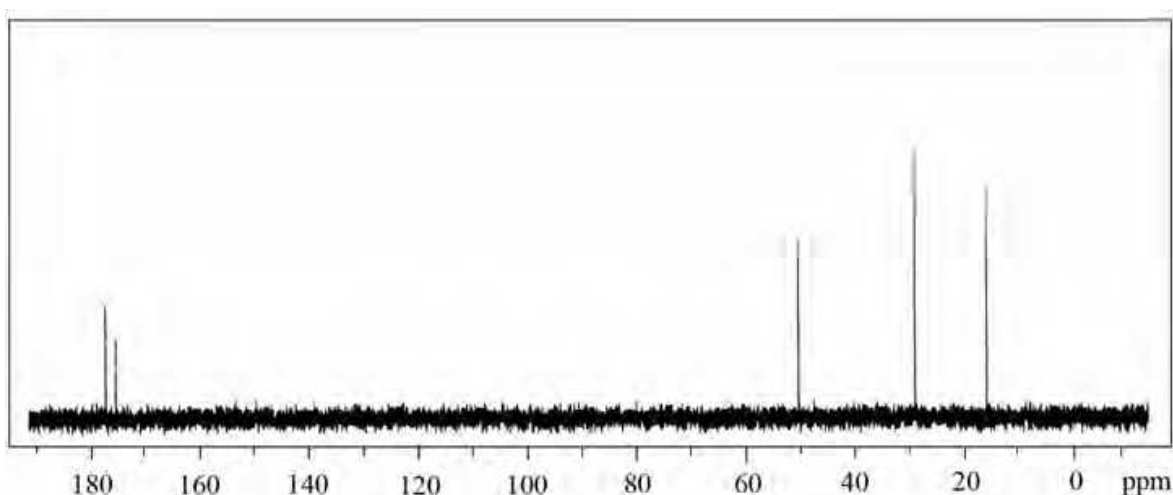


Fig. 6. ^{13}C -NMR spectrum of LAS crystal.

Spectra	Chemical Shift (ppm)	Group identification
^1H NMR	1.33	- CH_3 -
	2.57	- CH_2 -
	3.65	- CH -
	4.69	- D_2O
^{13}C -NMR	16.00	- CH_3
	29.06	- CH_2 -
	50.33	- CH -
	175.52	COOH of L-Alanine
	177.41	COOH of Succinic Acid

Table 4. The chemical shifts in ^1H -NMR and ^{13}C -NMR spectra of LAS.

10.2.6 Thermal analysis

The Thermo Gravimetric Analysis (TGA), Differential Thermal Analysis (DTA) spectra of grown LAS crystal have been obtained using the instrument NETSZCH SDT Q 600 V8.3 Build 101. The TGA and DTA have been carried out in nitrogen atmosphere at a heating rate of 20°C/min from 0°C to 1000°C. The TGA curve is presented in Fig. 7.

The initial mass of the materials to analysis was 2.5720 mg and the final mass left out after the experiment was only 1.729 % of initial mass. The TGA trace shows that the material exhibit very small weight loss of about 1.17 % in the temperature up to 155°C due to loss of water. TGA curve shows that there is the weight loss (85%) between 178°C and 274°C indicating that the decomposition of LAS crystals. From the Fig. 7, the appearance of endothermic in the DTA at 178°C corresponds to TGA results. From the TGA, DTA analyses, it is clearly understood that the LAS is thermally stable upto 178°C.

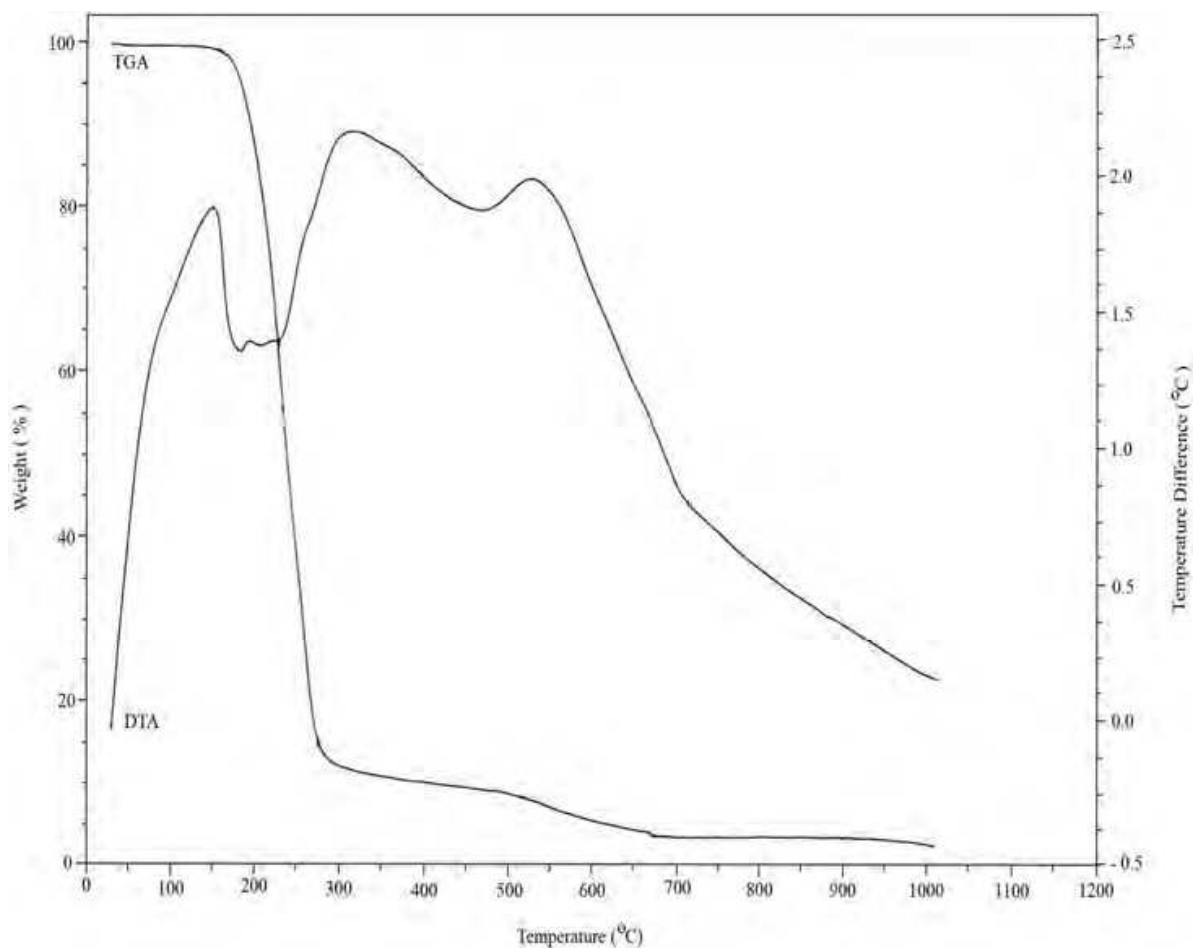


Fig. 7. TGA / DTA curve of LAS crystal.

10.2.7 Second harmonic generation analysis

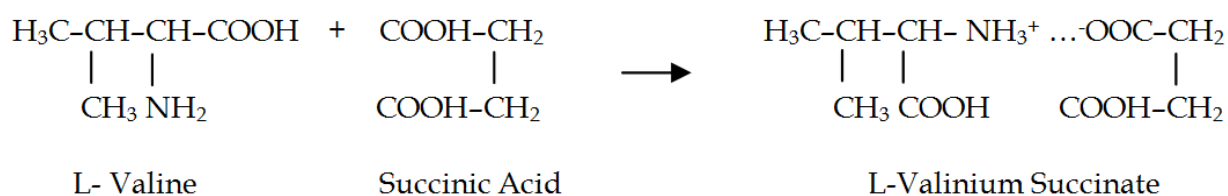
A preliminary study of the powder SHG measurement of LAS has been performed using Kurtz powder technique (Kurtz & Perry, 1968) with 1064nm laser radiations. An Nd:YAG laser producing pulses with a width of 8 ns and a repetition rate of 10 Hz was used. The crystal was crushed into powder and densely packed in a capillary tube. It is observed that the crystal converts the 1064 nm radiation into green (532 nm) while passing the Nd:YAG laser output into the sample which confirms the SHG. The observed intensity of output light

is obtained as 12 mV and for the same incident radiation, the output of KDP is observed as 52 mV. It was found that the efficiency of SHG is 23% when compared with that of the standard KDP (Ramachandra Raja , 2009c).

11. Growth and characterization of L- Valinium Succinate (LVS)

11.1 Experimental procedure

The nonlinear optical crystal L-Valinium Succinate (LVS) were grown by slow evaporation solution growth method. The LVS was synthesized from analar grade L-Valine and Succinic acid which were taken in equimolar ratio 1:1 using following reaction:



The calculated amounts of reactants were thoroughly dissolved in double distilled water and stirred continuously using magnetic stirrer. The saturated solution may contain impurities such as solid and dust particles and therefore it was filtered using filter paper. Then the filtered solution was covered by polythene paper in which 10 to 15 holes were made for slow evaporation. This solution was transferred to crystal growth vessels and crystallization was allowed to take place by slow evaporation at a temperature range of 35°C in a constant temperature bath of accuracy $\pm 0.01^\circ\text{C}$. As a result of slow evaporation of water, the excess of solute has grown as LVS crystals in the period of two weeks.

11.2 Characterization studies

11.2.1 Single crystal XRD analysis

The X-Ray diffraction pattern of LVS crystals have been studied by ENRAF NONIUS CAD4 single crystal X-Ray diffractometer with MoK α radiation ($\lambda=0.71069 \text{ \AA}$). The single crystal X-ray diffraction study of crystals is used to identify the cell parameters. It is observed that the LVS crystal belongs to orthorhombic system with following cell parameters: $a = 9.85 \text{ \AA}$, $b = 5.35 \text{ \AA}$, $c = 12.26 \text{ \AA}$ and $\alpha = \beta = \gamma = 90^\circ$, the cell volume = 646 \AA^3 . From the lattice parameters it is clear that for grown crystal $a \neq b \neq c$ and $\alpha = \beta = \gamma = 90^\circ$ and they are compared with powder XRD data and tabulated in Table 5.

XRD	a Å	b Å	c Å	α deg	β deg	γ deg	Volume Å ³
Single crystal	9.85	5.35	12.26	90	90	90	646
Powder	9.99	5.36	12.19	90	90	90	652

Table 5. The cell parameters of LVS crystal.

11.2.2 Powder XRD analysis

The powder X-ray diffraction (XRD) pattern of LVS crystals has been obtained using Rich Seifert X-ray diffractometer. The crushed powder sample was subjected to intense X-rays of wavelength 1.54060 \AA (CuK α) at a scan speed of $1^\circ/\text{minute}$. The powder X-ray pattern of LVS is shown in Fig. 8. The observed powder XRD pattern has been indexed by Rietveld Index software package. The lattice parameters have been calculated by Rietveld Unit Cell

software package and they are shown in Table 5. It is observed that LVS belongs to orthorhombic system and cell parameters values are agreed with the single crystal XRD data. The h, k, l values, d-spacing and 2θ values are tabulated in Table 6.

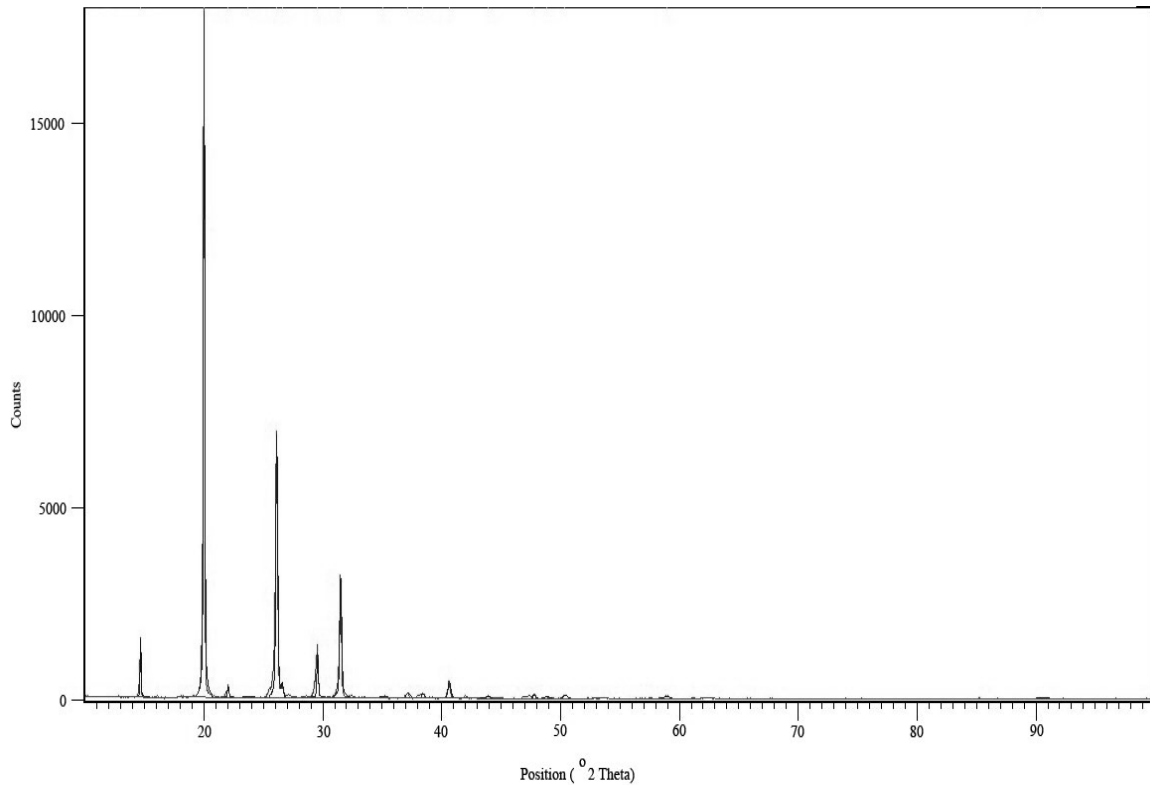


Fig. 8. Powder XRD pattern of LVS crystal.

Position $^{\circ}2\theta$	d- spacing Å	(h k l)
14.6613	6.04207	(0 0 2)
20.0051	4.43853	(0 2 1)
22.0352	4.03399	(1 0 2)
23.6856	3.75650	(0 1 3)
26.1127	3.41259	(1 2 1)
29.5373	3.02427	(0 0 4)
31.4841	2.84157	(0 3 2)
35.0908	2.55733	(0 3 3)
37.1320	2.42131	(2 0 2)
38.3887	2.34489	(2 2 0)
40.6179	2.22120	(1 0 5)
43.8867	2.06304	(1 3 4)
47.7577	1.90447	(1 0 6)
48.8085	1.86590	(2 2 4)
50.3581	1.81206	(1 4 4)
58.9110	1.56775	(3 3 0)
90.4585	1.08503	(2 2 10)

Table 6. Powder XRD data of LVS crystal.

11.2.3 UV-Vis-NIR analysis

To find the optical transmission range of LVS crystals, the UV-Vis-NIR spectrum has been recorded using Lambda 35 double beam spectrophotometer in the range between 190 nm and 1100 nm and it is shown in Fig. 9. When the transmittance is monitored from longer to shorter wavelengths, LVS is transparent from 190 nm to 1100 nm. Optical absorption with lower cut-off wavelength near 190 nm makes the crystal suitable for UV tunable laser and SHG device applications.

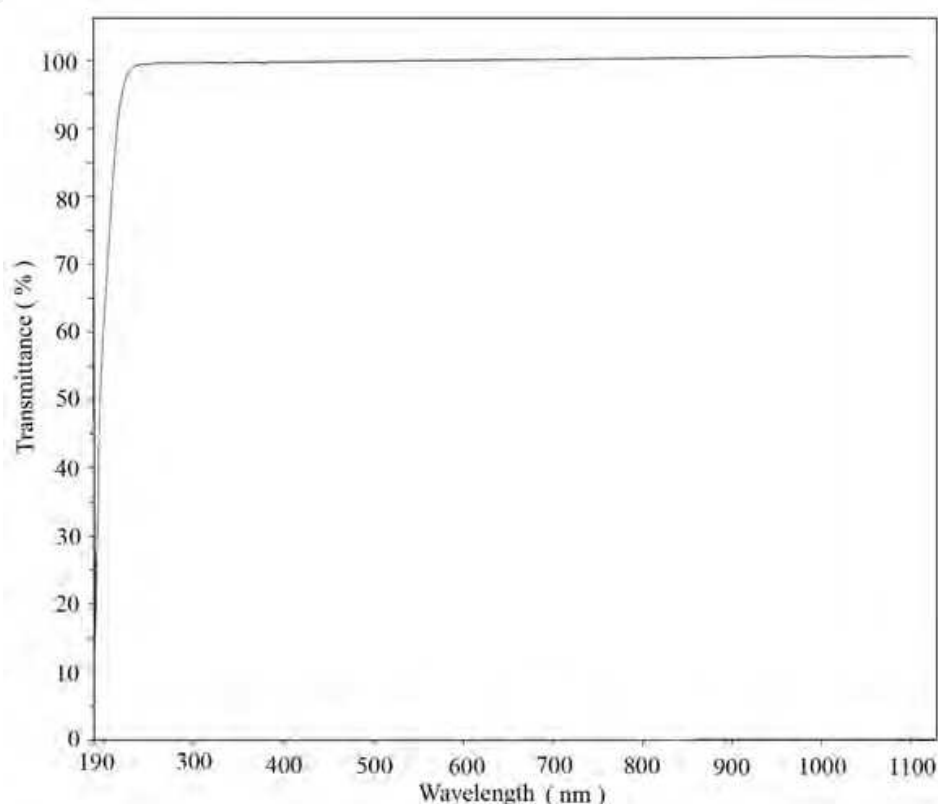


Fig. 9. UV-Vis-NIR spectrum of LVS crystal.

11.2.4 FT-IR analysis

The Fourier transform infrared spectrum of LVS have been recorded in between the region 400 - 4000 cm^{-1} using Perkin Elmer Fourier transforms infrared spectrometer (model SPECTRUM RX1) with the help of KBr pellets as shown in Fig. 10. The presence of functional groups was identified and they are stacked in Table 7. The presence of NH_3^+ group in LVS has confirmed by peaks at 3429 cm^{-1} and 3156 cm^{-1} . It is due to protonation of NH_2 group by the COOH group of succinic acids (Nakamo, 1978; Sajan et al., 2004). The symmetric and asymmetric bending of NH_3^+ was obtained at 1587 and 1508 cm^{-1} respectively. The strong absorption at 1393 cm^{-1} indicates that the symmetric bending of CH_2 . The CH_2 wagging vibration produces a sharp peak at 1327 cm^{-1} . The C-CH bending vibration produced its characteristic peak at 1270 cm^{-1} . The rocking vibration at 1177 cm^{-1} establishes the presence NH_3^+ group. The peak at around 1137 cm^{-1} is assigned to NH_3^+ wagging. The stretching vibration of C-O-C, C-C-N and C-C are positioned at 2108 cm^{-1} , 1063 cm^{-1} and 1029 cm^{-1} respectively. Meanwhile, for the peaks at 945 cm^{-1} is due to CH_2

rocking. The bending vibration of COO^- is observed at 662 cm^{-1} . The bending and rocking vibration of COO^- are observed at 714 cm^{-1} and 430 cm^{-1} respectively.

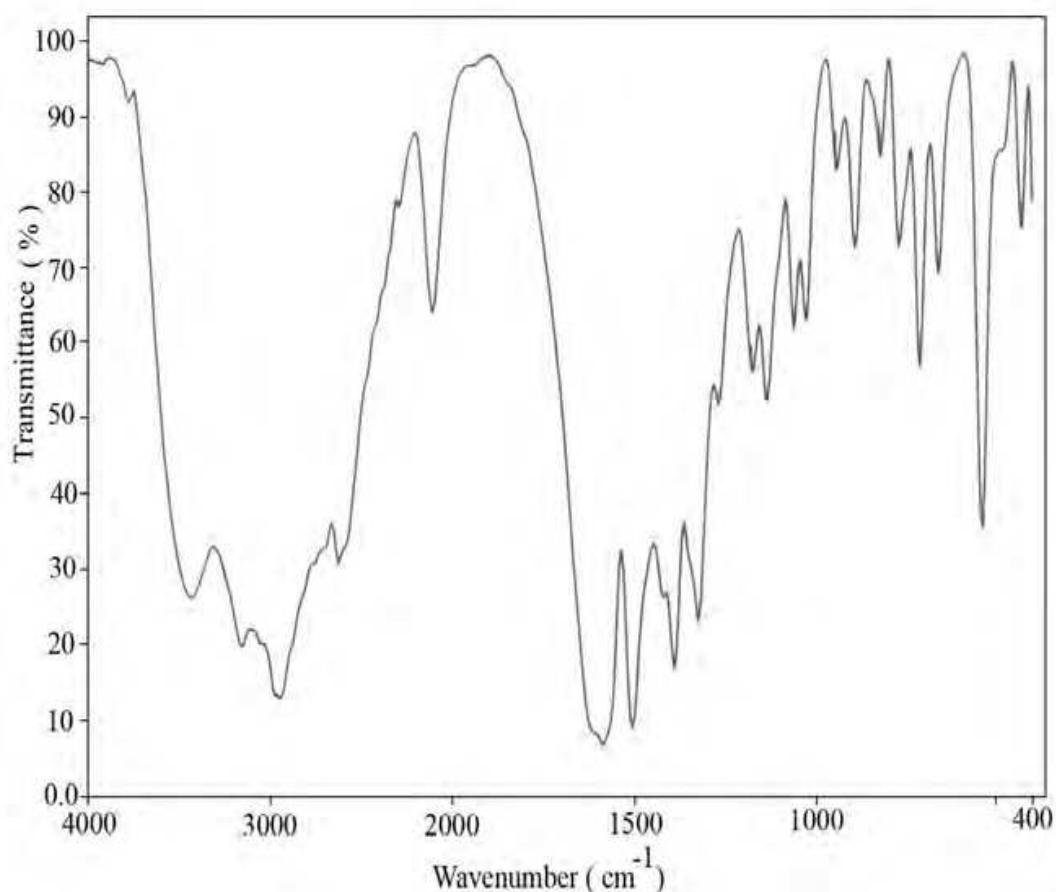


Fig. 10. FT-IR spectrum of LVS crystal.

11.2.5 NMR studies

The ^1H - and ^{13}C -NMR spectra of LVS have been recorded for the crystals dissolved in water (D_2O) using BRUKER 300 MHz (Ultrasield)TM instrument at 23°C (300 MHz for ^1H -NMR and 75 MHz for ^{13}C -NMR) for the confirmation of molecular structure. The ^1H - NMR spectrum of LVS is shown in the Fig. 11. The deuterium exchange proton NMR spectrum of LVS crystal is found to contain resonance signals integrated for a total of 12 protons. From the spectrum, it is observed that the two methyl proton signal is split into two doublets due to the coupling of neighbouring ($-\text{CH}$) proton which is confirmed from the signal at $\delta = 0.84\text{ ppm}$, $\delta = 0.89\text{ ppm}$ respectively. The $-\text{CH}$ group signal is split into a multiplet due to the hyperfine splitting of neighbouring three ($-\text{CH}_3$) protons is confirmed from the signal of LVS crystal centered at $\delta = 2.13\text{ ppm}$. The doublet signal observed at $\delta = 3.48\text{ ppm}$ is attributed to a ($-\text{CH}$) proton next to carboxylic acid. There is one peak found at $\delta = 2.51\text{ ppm}$ due to the $-\text{CH}_2-$ group of succinic acid. The signal at $\delta = 4.69\text{ ppm}$ is due to the solvent D_2O . The signals due to N-H and COOH do not show up because of fast deuterium exchanges which took place in those two groups, where the D_2O was used as the solvent (Bruice 2002). The chemical shift values of LVS with assignments are tabulated in Table 8.

Wavenumber (cm^{-1})	Assignment
3429	NH_3^+ symmetric stretching
3156	NH_3^+ asymmetric stretching
2946	CH_2 asymmetric stretching
2626	NH_3^+ symmetric stretching
2108	C-O-C stretching
1587	NH_3^+ symmetric bending
1508	NH_3^+ asymmetric bending
1393	CH_2 symmetric bending
1327	CH_2 wagging
1270	C-CH bending
1177	NH_3^+ rocking
1137	NH_3^+ wagging
1063	C-C-N stretching
1029	C-C stretching
945	CH_2 rocking
893	C-C-N stretching
823	COO^- rocking
773	NH wagging
714	COO^- bending
662	COO^- bending
541	C-C=O wagging
430	COO^- rocking

Table 7. Assignments of FT-IR bands observed for LVS crystal.

The ^{13}C -NMR spectrum is shown in Fig. 12. The characteristic absorption peaks of ^{13}C -NMR spectrum of LVS are explained as follows. The signals at $\delta = 17.82$ ppm and $\delta = 16.55$ ppm are attributed to the two methyl group of LVS. An intense signal is observed at $\delta = 28.93$ ppm is due to presence of two methylene groups of succinic acid. The signal of (CH) at $\delta = 29.00$ ppm is integrated for one carbon due to presence of carboxylic acid isopropyl carbon. The peaks at $\delta = 60.12$ ppm is due to tertiary carbon connected to amino group. The peak at $\delta = 173.97$ ppm and $\delta = 177.28$ ppm are due to deuterium exchange of carbon in carbonyl group. A peak with higher intensity at $\delta = 177.28$ ppm can be safely attributed to carbonyl carbons of two COOH groups of succinic acid present in the same chemical environment.

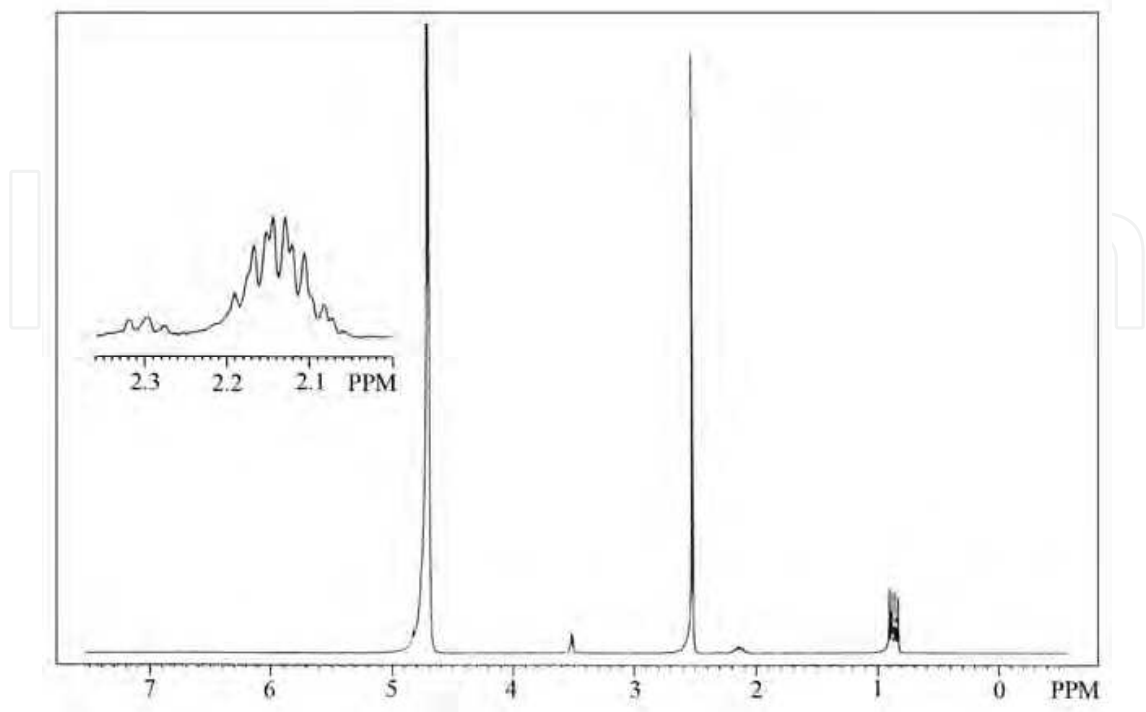


Fig. 11. $^1\text{H-NMR}$ spectrum of LVS crystal.

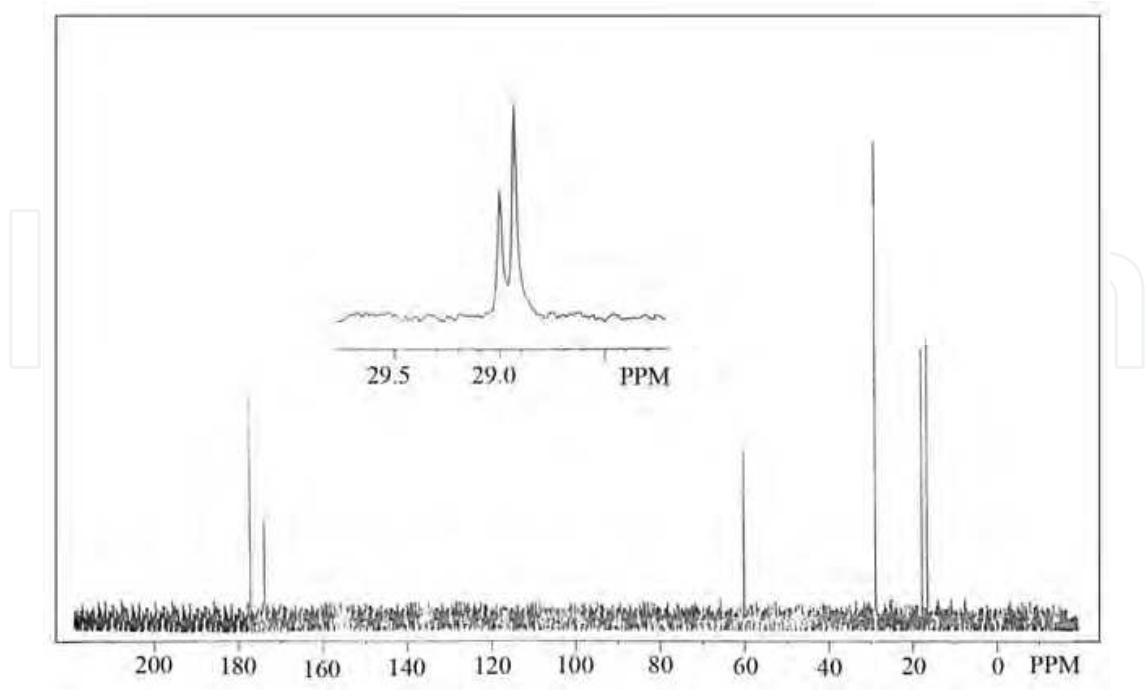


Fig. 12. $^{13}\text{C-NMR}$ spectrum of LVS crystal.

Spectra	Chemical Shift (ppm)	Group identification
^1H NMR	0.84 & 0.89	- (CH ₃) -
	2.13	- CH -
	2.51	- CH ₂ -
	3.48	- CH -
	4.69	D ₂ O
^{13}C -NMR	16.55 & 17.82	- (CH ₃) -
	29.00	- CH -
	28.93	- CH ₂ -
	60.12	- CH -
	173.97	COOH of L-Valine
	177.28	COOH of Succinic Acid

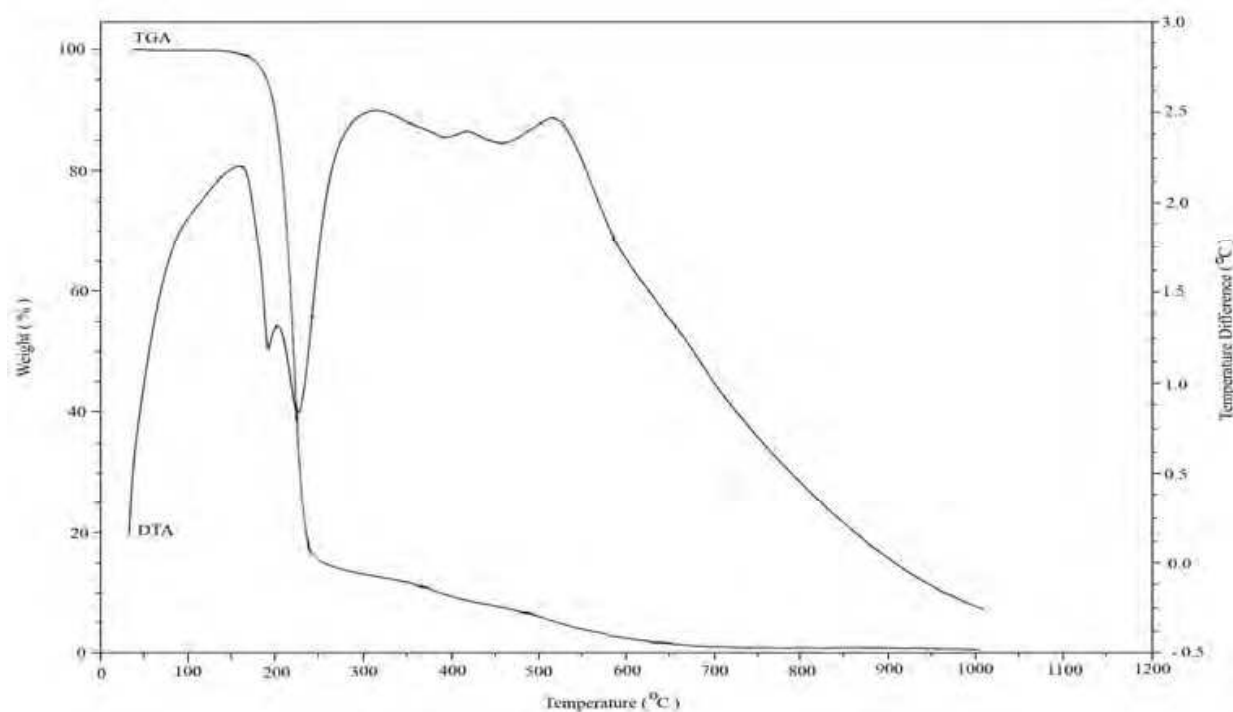
Table 8. The chemical shifts in ^1H -NMR and ^{13}C -NMR spectra of LVS.

Fig. 13. TGA / DTA curve of LVS crystal.

11.2.6 Thermal analysis

The Thermo Gravimetric Analysis (TGA), Differential Thermal Analysis (DTA) spectra of grown LVS crystal have been obtained using the instrument NETSZCH SDT Q 600 V8.3 Build 101. The TGA and DTA have been carried out in nitrogen atmosphere at a heating rate of 20°C/min from 0°C to 1000°C. The TGA curve is presented in Fig. 13. The initial mass of the materials to analysis was 3.0160 mg and the final mass left out after the experiment was only 0.8631 % of initial mass.

The TGA trace shows that the material exhibit very small weight loss of about 1.04 % in the temperature up to 160°C due to loss of water. TGA curve shows that there is a weight loss of about 92 % between 160°C to 500°C indicating that the decomposition of LVS crystals. From the Fig. 13, the appearance of sharp endothermic in the DTA at 222°C corresponds to TGA results. From the TGA, DTA analyses, it is clearly understood that the LVS is thermally stable upto 222°C.

11.2.7 Second harmonic generation analysis

The nonlinear optical susceptibility of grown LVS crystals have been measured through second harmonic generation using standard Kurtz and Perry method (Kurtz & Perry, 1968). The output of laser beam having the bright green emission of wavelength 532 nm confirms the second harmonic generation output. The observed intensity of output light is 31 mV. For the same incident radiation, the output of KDP was observed as 55 mV. The second harmonic efficiency of LVS is 0.56 times that of KDP.

12. Conclusions

Thus the chapter fully discussed about solution crystal growth methods and nucleation. Then the growth and characterization of Single crystals of L- Alaninium Succinate (LAS) and L-Valinium Succinate (LVS) have been grown by slow evaporation method from saturated solution are also discussed. From X-Ray diffraction, it is observed that LAS and LVS crystal belongs to orthorhombic system. The UV-Vis-NIR spectral studies confirm that the grown crystals have wider transparency range in the visible and UV spectral regions and both LAS and LVS crystals have lower cut-off at 190 nm. The good transparency shows that LAS and LVS crystal can be used for nonlinear optical applications. The modes of vibration of the molecules and the presence of functional groups have been identified using FT-IR technique. The chemical structure of the grown crystals is established by ¹H and ¹³C NMR techniques. From Thermal analysis, the melting point of LAS and LVS are identified is 178 °C and 222°C respectively. The SHG output proves that LAS and LVS crystals can be used as nonlinear optical materials.

13. Acknowledgment

The authors thank Dr. P.K. Das, Indian Institute of Science, Bangalore for the measurement of powder SHG efficiency. The authors are thankful to St. Joseph's College, Trichy, India, and SASTRA University, Thanjavur, India and Central Electro Chemical Research Institute (CECRI), Karaikudi, India for spectral facilities. The authors also express their gratitude to, Indian Institute of Technology, Chennai, India for XRD facilities

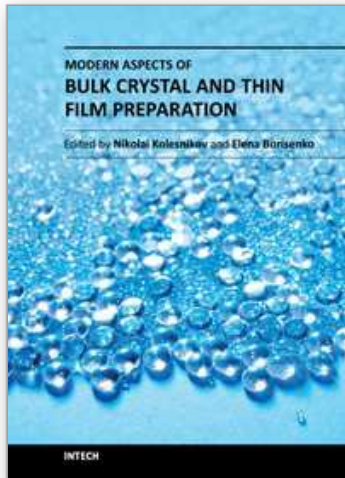
14. References

- Aravindan, A., Srinivasan, P., Vijayan, N., Gopalakrishnan, R., & Ramasamy P. (2007). Investigations on the growth, optical behaviour and factor group of an NLO crystal: L-alanine alaninium nitrate. *Cryst. Res. Technol.*, Vol. 42, No.11, (November 2007), pp. 1097-1103, ISSN 0232-1300
- Brice, J.C. (January 1987). *Crystal Growth Processes*, John Wiley and Sons, ISBN 0-470-20268-8, New York.
- Bruice P.Y. (2002). *Organic Chemistry*, Pearson Education Pvt. Ltd, Singapore.
- Buckley H.E. (4 May 1951). *Crystal Growth*, Wiley, New York.
- Chenthamarai, S., Jayaraman, D., Ushasree, P.M., Meera, K., Subramanian, C., & Ramasamy P. (2000). Experimental determination of induction period and interfacial energies of pure and nitro doped 4-hydroxyacetophenone single crystals. *Mater. Chem. Phys.*, Vol. 64, No. 3, (May 2000), pp. 179-183, ISSN 0254-0584
- Dhanuskodi, S., & Vasantha, K. (2004). Structural, thermal and optical characterizations of a NLO material: L-alaninium oxalate. *Cryst. Res. Technol.*, Vol. 39, No. 3, (March 2004), pp. 259-265, ISSN 0232-1300
- Dhanuskodi, S., Vasantha, K., & Angeli Mary, P.A. (2007). Structural and thermal characterization of a semiorganic NLO material: l-alanine cadmium chloride. *Spectrochim. Acta A* , Vol. 66, No. 3, (March 2007) pp. 637-642, ISSN 1386-1425
- Eimerl, D., Velsko, S., Davis, L., & Wang, F. (1990). Progress in nonlinear optical materials for high power lasers. *Prog. Cryst. Growth Charact.*, Vol. 20, No. 1, pp. 59-113, ISSN 0960-8974
- Kurtz, S.K., & Perry, T.T. (1968). A Powder Technique for the Evaluation of Nonlinear Optical Materials. *J. Appl. Phys.*, Vol. 39, pp.3798 - 3813, ISSN 0021-8979
- Milton , B., Boaz, Leyo Rajesh, A., Xavier Jesu Raja, S., & Jeromedas S. (2004). Growth and characterization of a new nonlinear optical semiorganic lithium paranitrophenolate trihydrate ($\text{NO}_2\text{-C}_6\text{H}_4\text{-OLi}\cdot 3\text{H}_2\text{O}$) single crystal. *J. Cryst. Growth*, Vol. 262, pp. 531-535, ISSN 0022-0248
- Natarajan, S., Shanmugam, G., and Martin Britto Dhas, S.A. (2008), Growth and characterization of a new semi organic NLO material: L-tyrosine hydrochloride', *Cryst. Res. Technol.*, Vol. 43, pp. 561-564.
- Ramachandra Raja, C. & Antony Joseph, A. (2009) Crystal growth and characterization of new non linear optical single crystals of L- alaninium fumarate. *Materials Letters*, Vol. 63, No. 28 (November 2009) 2507- 2509, ISSN 0167-577X
- Ramachandra Raja, C. & Antony Joseph, A. (2009). Crystal growth and comparative studies of XRD, spectral studies on new NLO crystals: L- valine and L- valinium succinate. *Spectrochim. Acta. A*, Vol. 74, No. 3 (October 2009), pp. 825-828, ISSN1386-1425
- Ramachandra Raja, C., Gokila, G. & Antony Joseph, A. Growth and spectroscopic characterization of a new organic nonlinear optical crystal: L-alaninium succinate. *Spectrochim. Acta. A* Vol. 72, No. 4, (May 2009) pp. 753-756, ISSN1386-1425

Ramachandra Raja, C, & A. Antony Joseph (2010). Synthesis, spectral and thermal studies of new nonlinear optical crystal: L-valinium fumarate. *Materials Letters* Vol. 64, No.2. (January 2010), pp. 108-110, ISSN 0167-577X

IntechOpen

IntechOpen



Modern Aspects of Bulk Crystal and Thin Film Preparation

Edited by Dr. Nikolai Kolesnikov

ISBN 978-953-307-610-2

Hard cover, 608 pages

Publisher InTech

Published online 13, January, 2012

Published in print edition January, 2012

In modern research and development, materials manufacturing crystal growth is known as a way to solve a wide range of technological tasks in the fabrication of materials with preset properties. This book allows a reader to gain insight into selected aspects of the field, including growth of bulk inorganic crystals, preparation of thin films, low-dimensional structures, crystallization of proteins, and other organic compounds.

How to reference

In order to correctly reference this scholarly work, feel free to copy and paste the following:

A. Antony Joseph and C. Ramachandra Raja (2012). Growth of Organic Nonlinear Optical Crystals from Solution, Modern Aspects of Bulk Crystal and Thin Film Preparation, Dr. Nikolai Kolesnikov (Ed.), ISBN: 978-953-307-610-2, InTech, Available from: <http://www.intechopen.com/books/modern-aspects-of-bulk-crystal-and-thin-film-preparation/growth-of-organic-nonlinear-optical-crystals-from-solution>

INTECH
open science | open minds

InTech Europe

University Campus STeP Ri
Slavka Krautzeka 83/A
51000 Rijeka, Croatia
Phone: +385 (51) 770 447
Fax: +385 (51) 686 166
www.intechopen.com

InTech China

Unit 405, Office Block, Hotel Equatorial Shanghai
No.65, Yan An Road (West), Shanghai, 200040, China
中国上海市延安西路65号上海国际贵都大饭店办公楼405单元
Phone: +86-21-62489820
Fax: +86-21-62489821

© 2012 The Author(s). Licensee IntechOpen. This is an open access article distributed under the terms of the [Creative Commons Attribution 3.0 License](#), which permits unrestricted use, distribution, and reproduction in any medium, provided the original work is properly cited.

IntechOpen

IntechOpen